Springer

KSME

Journal of Mechanical Science and Technology 24 (11) (2010) 2315~2321
www.springerlink.com/content/1738-494x
DOI 10.1007/s12206-010-0813-6

Compliant actuation of parallel-type variable stiffness actuator based on antagonistic actuation †

Ki-Hoon Nam, Byeong-Sang Kim and Jae-Bok Song*

School of Mechanical Engineering, Korea University, Seoul, 137-713, Korea

(Manuscript Received November 10, 2009; Revised May 29, 2010; Accepted July 19, 2010)

Abstract

For a service robot requiring physical human-robot interaction, stable contact motion and collision safety are very important. To accomplish these functions, we propose a novel design for a parallel-type variable stiffness actuator (PVSA). The stiffness and position of a joint can be controlled simultaneously using the PVSA based on an antagonistic actuation inspired by the musculoskeletal system. The PVSA consists of a dual-cam follower mechanism, which acts like a human muscle, and a drive module with two motors. Each cam placed inside the dual cam-follower mechanism has two types of cam profile to provide a wide range of stiffness variation and collision safety. The use of the PVSA enables position and stiffness control to occur simultaneously. Furthermore, joint stiffness instantly decreases when the PVSA is subject to a high torque exceeding a pre-determined value, thereby improving collision safety. Experiments showed that the PVSA provides effective levels of variable stiffness and collision safety.

Keywords: Variable stiffness; Antagonistic actuation; Dual cam-follower mechanism; Collision safety

1. Introduction

Although force control can be achieved by a conventional robot manipulator [1], some problems can occur. For example, the lowest stiffness of a manipulator for compliant motion is limited due to friction in the mechanical parts and the time delay during the communication between the robot and controller. Also, the rigid structure of a conventional robot can threaten a human or its environment. These issues have motivated the design of a new joint actuation mechanism for service robots.

A variable stiffness joint mechanism that provides simultaneous control of position and stiffness is considered to be an effective solution. Many ideas for variable stiffness joint mechanisms have been proposed and can be divided into two categories. The first idea is an antagonistic mechanism inspired by the musculoskeletal system [2-7]. A pair of actuators connected to the same joint through nonlinear springs exerts torque antagonistically to control both position and stiffness. The variable stiffness actuator (VSA) in [3] is the representative example in this approach. The four bar linkages with torsion springs were adopted to replace the nonlinear springs. The second idea is a serial actuation composed of a motor for position control and a variable stiffness mechanism, which is connected to the position frame in series [8-14]. The variable stiffness joint designed at DLR is the representative example in this approach. The cam-follower mechanism was used for stiffness variation and the joint stiffness could be controlled by adjusting the compression length of a linear spring [10].

By using these variable stiffness actuators, simultaneous control of position and stiffness, which is advantageous to dexterous manipulation, can be achieved. In addition, compliant motion, which is good for collision safety, can be provided. The previous variable stiffness actuators require considerable time to vary the joint stiffness, even though most collisions occur in an instant. Compared to a rigid joint, the variable stiffness actuator is relatively safe but not intrinsically safe.

To address this problem, a novel design for a parallel-type variable stiffness actuator (PVSA) based on antagonistic actuation with a collision safety function is proposed. The PVSA consists of a dual cam-follower mechanism and a drive module with two motors. One-half of the dual cam-follower mechanism (i.e., a single cam-follower mechanism) with a linear spring acts as a single nonlinear spring in the antagonistic actuation mechanism. The two cams used in the dual cam-follower mechanism are independently actuated by two motors. Control of each cam enables simultaneous control of position and stiffness.

The PVSA has two main functions: antagonistic actuation and collision safety. The linear and curved cam profiles are

† This paper was recommended for publication in revised form by Associate Editor Jong Hyeon Park

* Corresponding author. Tel.: +82 2 3290 3363, Fax: +82 2 3290 3757
E-mail address: jbsong@korea.ac.kr

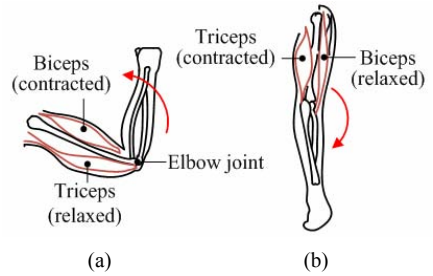

Fig. 1. Antagonistic mechanism of human arm: (a) flexion and (b) extension.

partially adopted in each cam for two main functions of the PVSA. The antagonistic actuation mode is activated until the applied torque is smaller than the threshold torque. If the applied torque is larger than the threshold torque, the collision safety mode is activated and the joint stiffness greatly decreases to absorb the collision force. These features of the PVSA are advantageous to service robots.

The remainder of this paper is organized as follows: Section II describes the concept of an antagonistic actuation. Section III explains the principles of the PVSA. The prototype and experimental results are shown in Section IV. The collision safety is described in Section V. Finally, our conclusions are given in Section VI.

2. Antagonistic actuation

Antagonistic actuation consists of a joint and two power sources. For example, the elbow of a human is controlled by the biceps and triceps muscles. Position and stiffness of the elbow are controlled by adjusting their lengths. Flexion (Fig. 1(a)) occurs when the biceps contracts and the triceps relaxes, and extension (Fig. 1(b)) is achieved in the opposite manner. On the other hand, the stiffness of the elbow increases when both the biceps and the triceps contract at the same time.

Antagonistic actuation can be realized by a mechanical system composed of two links and two nonlinear springs, as shown in Fig. 2. Assume that the rotation of links 1 and 2 can be independently controlled, and both springs are initially compressed to θ_1 and θ_2. This initial compression delivers compressive forces to the output link throughout their operation range at all times. The stiffness of the joint is associated with the spring forces controlled by the two links. Suppose that the output link passively rotates by $\Delta\theta_p$ due to external force F_e, and reactive torque τ_p is generated by the extension of spring 1 and the compression of spring 2 (Fig. 2(a)). Assume that links 1 and 2 rotate counter-clockwise (CCW) and clockwise (CW) by $\Delta\theta_1$ and $\Delta\theta_2$, respectively, so that both springs are further compressed as shown in Fig. 2(b). This will increase the stiffness of the joint, which leads to a new curve for τ-θ_p as shown in Fig. 2(b). Compared to the low stiffness situation, a much higher torque ($\tau'_p > \tau_p$) is required to rotate the output link by the same angular displacement $\Delta\theta_p$ in this preloaded state, which means that high joint stiffness is achieved.

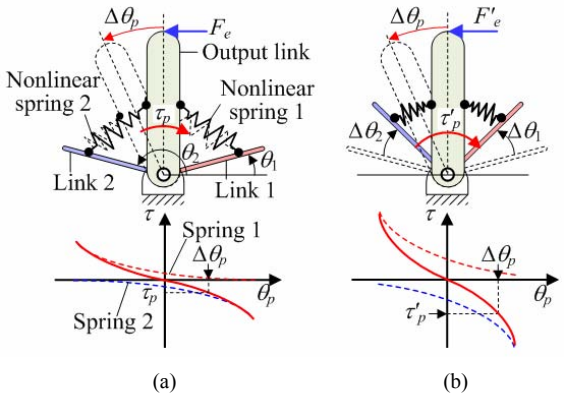

Fig. 2. Mechanical antagonistic actuation system: (a) initial state (low joint stiffness) and (b) preloaded state (high joint stiffness).

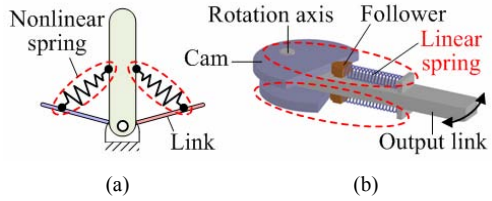

Fig. 3. Dual cam-follower mechanism of PVSA: (a) schematic diagram of antagonistic actuation and (b) antagonistic mechanism based on dual cam-follower mechanism.

3. Design of PVSA

3.1 Dual cam-follower mechanism of PVSA

A pair of nonlinear springs is required to construct an antagonistic mechanism as illustrated in Fig. 3(a). However, the selection of commercially available nonlinear springs is very limited, and the design of a proper nonlinear spring for antagonistic actuation is complicated. Therefore, a dual cam-follower mechanism was adopted in the proposed PVSA as shown in Fig. 3(b). Two symmetric cams were placed on the top and bottom sides of the joint, and they contact each follower connected to the output link via linear springs. The combination of a linear spring and a cam-follower mechanism functions as a nonlinear spring in the antagonistic mechansim.

The antagonistic actuation modes of the PVSA can be classified into three cases: position control, stiffness control, and simultaneous position and stiffness control. The position and stiffness depend on the rotation angles of cam 1 and 2. The position difference ϕ of cam 1 and 2, shown in Fig. 4, causes the stiffness variation. When the rotation angles of cam 1 and 2 are identical in size but opposite in direction as depicted in Figs. 4(a) and (b), only the joint stiffness changes (i.e., stiffness control). On the other hand, if cam 1 and 2 rotate with an identical angle in one direction, the output link also rotates in that direction as shown in Fig. 4(c) while the stiffness is kept constant (i.e., position control). Furthermore, simultaneous position and stiffness control can be achieved when cam 1 and 2 have different rotation angles as shown Fig. 4(d).

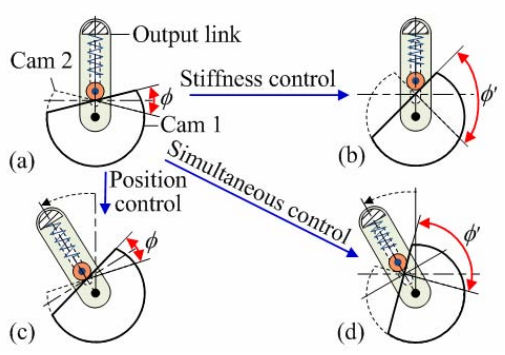

Fig. 4. Antagonistic actuation of dual cam-follower mechanism: (a) low stiff condition, (b) high stiffness condition, (c) position control and (d) simultaneous position and stiffness control.

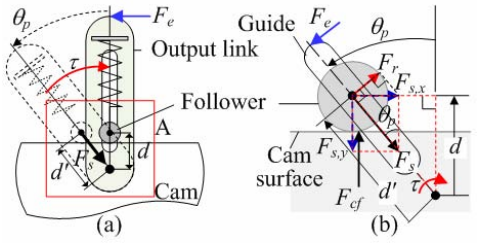

Fig. 5. Cam-follower mechanism of PVSA: (a) nonlinear torque generation and (b) free body diagram of follower (enlarged view of A).

3.2 Cam analysis

The dual cam-follower mechanism is symmetric, so only one-half of the mechanism was needed to analyze its basic characteristics. As shown in Fig. 5(a), one-half of the dual cam-follower mechanism of the PVSA consists of the cam-follower module with a linear spring, and an output link including a guide for the linear motion of a follower. The follower always maintains contact with the cam since the spring is initially compressed by l_{preset}. The application of the external force F_e to the end of the output link generates a passive deflection θ_p, which is defined by the angle between the output link and the normal direction of the cam surface. Then, the reactive torque τ is generated by the compressive force of the spring as shown in Fig. 5.

As the passive deflection angle θ_p increases, the spring is nonlinearly compressed. Assume that d and d' are the initial and final positions of the follower, respectively; then, the compression Δd (= d'–d) can be obtained from the geometric relationship as shown in Fig. 5(b). Because d' equals $d \cdot \sec\theta_p$, the spring force F_s can be derived as

$$F_s = k_s(l_{preset} + \Delta d) = k_s\{l_{preset} + d(\sec\theta_p - 1)\} \tag{1}$$

where k_s is the spring constant and l_{preset} is the initial compression of the spring.

The spring force is converted to the reactive force F_r in the direction normal to the guide at the output link. Since spring force in the y-direction $F_{s,y}$ is cancelled out by the reactive force applied from the cam to the follower F_{cf}, the reactive force F_r is given by

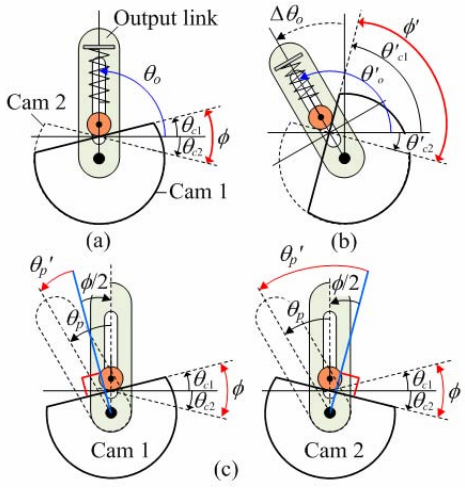

Fig. 6. Schematic diagram of PVSA: (a) initial state, (b) simultaneous position and stiffness control and (c) separated dual cam-follower mechanism for calculating τ_1 and τ_2.

$$\begin{aligned} F_r &= F_{s,x}\cos\theta_p \\ &= k_s\{l_{preset} + d(\sec\theta_p - 1)\}\sin\theta_p\cos\theta_p \end{aligned} . \tag{2}$$

Thus, the joint torque is obtained by

$$\tau = -d' \times F_r = -d\,k_s\{l_{preset} + d(\sec\theta_p - 1)\}\sin\theta_p . \tag{3}$$

3.3 Position and stiffness control of PVSA

The position and stiffness of the joint can be calculated by the rotation angles of cam 1 and 2. Fig. 6(a) shows the initial state of the PVSA. The angles θ_o, θ_{c1}, and θ_{c2} denote the rotation angle of the output link, cam 1, and cam 2, respectively. Assume that cam 1 and 2 rotate by θ'_{c1} and θ'_{c2}, respectively. Then, the output link rotates by θ_o' and the position difference of cam 1 and 2, ϕ (=$|\theta_{c1}-\theta_{c2}|$), changes to ϕ' as illustrated in Fig. 6(b). The position of the output link depends on an average of θ_{c1} and θ_{c2} with an offset of 90°; thus, it can be represented by

$$\theta_o = \frac{\theta_{c1} + \theta_{c2}}{2} + \frac{\pi}{2} . \tag{4}$$

On the other hand, the joint stiffness increases when the angle between the output link and the tangent of the cam profile at the contact point decreases, as explained in Sec. 3.2. That is, the joint stiffness depends on the position difference ϕ of the two cams.

The joint stiffness of the PVSA is obtained by differentiating the sum of τ_1 and τ_2, which represent the nonlinear joint torques corresponding to θ_p generated by cams 1 and 2, respectively. When cam 1 and 2 rotate by θ_{c1} and θ_{c2}, respec-

tively, the position of the output link is biased to -ϕ/2 and ϕ/2, respectively, as shown in Fig. 6(c).

Suppose that the output link passively rotates due to the external force. θ_p from Eq. (3) can be replaced with (θ_p-ϕ/2) and (θ_p+ϕ/2) for cam 1 and cam 2, respectively. Thus, joint torques τ_1 and τ_2 can be derived as

$$\begin{cases} \tau_1 = -d\,k_s\{l_{preset} + d(\sec(\theta_p - \frac{\phi}{2}) - 1)\}\sin(\theta_p - \frac{\phi}{2}) \\ \tau_2 = -d\,k_s\{l_{preset} + d(\sec(\theta_p + \frac{\phi}{2}) - 1)\}\sin(\theta_p + \frac{\phi}{2}) \end{cases} \quad (5)$$

We note that the signs of τ_1 and τ_2 are opposite when θ_p is smaller than ϕ/2 since the dual cam-follower mechanism works antagonistically. Given the sum of τ_1 and τ_2, the joint torque of the PVSA can be obtained by

$$\begin{aligned} \tau_{PVSA} = &-d\,k_s l_{preset}(\sin(\theta_p - \tfrac{\phi}{2}) + \sin(\theta_p + \tfrac{\phi}{2})) \\ &- d^2 k_s\{(\sec(\theta_p - \tfrac{\phi}{2}) - 1)\sin(\theta_p - \tfrac{\phi}{2}) \\ &+ (\sec(\theta_p + \tfrac{\phi}{2}) - 1)\sin(\theta_p + \tfrac{\phi}{2})\}. \end{aligned} \quad (6)$$

Finally, the joint stiffness of the PVSA corresponding to the passive deflection angle can be achieved by differentiating Eq. (6) as follows:

$$\begin{aligned} k_{PVSA} = &(k_s\,d^2 - k_s\,d \cdot l_{preset})\{\cos(\theta_p - \tfrac{\phi}{2}) \\ &+ \cos(\theta_p + \tfrac{\phi}{2})\} - k_s\,d^2\{\tan^2(\theta_p - \tfrac{\phi}{2}) \\ &+ \tan^2(\theta_p + \tfrac{\phi}{2}) + 2\}. \end{aligned} \quad (7)$$

Eq. (7) indicates that the joint stiffness is a function of θ_p and ϕ. If there is no external force (or torque), θ_p becomes zero. In this case, k_{PVSA} from Eq. (7) represents the initial joint stiffness of the PVSA when the position difference of the two cams is ϕ.

4. Prototype of the PVSA

4.1 Structure of variable stiffness module

The PVSA is composed of an antagonistic-type variable stiffness module based on the dual cam-follower mechanism and a drive module containing two motors, as shown in Fig. 7. The variable stiffness module consists of two cams and a middle plate. As illustrated in Fig. 7(c), two independent follower mechanisms including a follower, a guide, and four linear coil springs are installed inside of the middle plate, and they act as nonlinear springs with cam 1 and cam 2. Two internal ring gears, which are beneficial to the compact design of the PVSA, are used to connect the variable stiffness module to the drive module. One is connected to cam 1 via the housing, and the other is directly connected to cam 2. Therefore, the torques of motors 1 and 2 are independently transmitted to cams 1 and 2, respectively. The diameter and length of the PVSA are 92 mm and 60 mm, respectively, and its weight is 980 g without the two motors.

Table 1. Specifications of PVSA.

Size (without motors)	92 mm (D) x 60 mm (L)
Size (including motors)	92 mm (D) x 180 mm (L)
Weight	980 g
Stiffness variation range	0 ~ 0.9 Nm/°
Passive deflection angle	± 55° (at the lowest stiffness)
Switching time	700 ms

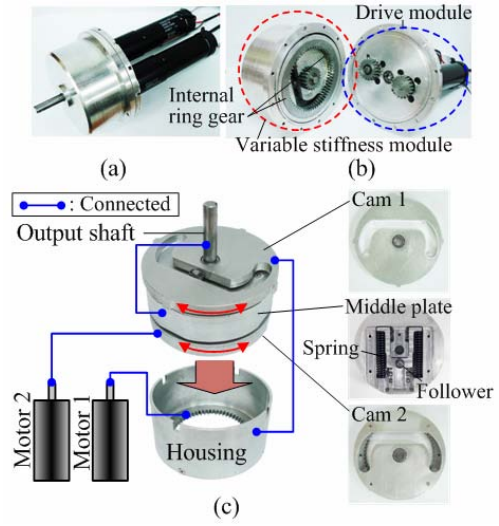

Fig. 7. Prototype of PVSA: (a) assembled PVSA, (b) disassembled PVSA and (c) internal parts of variable stiffness module.

The specifications of the PVSA are listed in Table 1. In antagonistic actuation, the maximum passive deflection angle θ_p of the PVSA is ±55° at the lowest joint stiffness, and it decreases as the joint stiffness increases.

4.2 Experiments on variable stiffness

Fig. 8 shows the experimental setup used to investigate the performance of the PVSA. The output link is connected to the output shaft of the PVSA through an F/T sensor. As the output link rotated due to the external force, the joint torque of the PVSA and the rotation angle of the output link were simultaneously measured by the force/torque sensor and the external encoder connected to the output shaft, respectively.

Fig. 9 shows the relationship between the output torque and the passive deflection angle when the position difference ϕ of cams 1 and 2 varied at intervals of 20° from 0° to 100°, respectively. In the high stiffness region, the measured joint torque showed good agreement with the theoretical torque obtained from Eq. (6), but some errors between them were observed in the low stiffness region. A small amount of hysteresis was also observed when the direction of the applied torque changed. These problems appear to be related to the friction force occurring in the internal parts of the variable stiffness module.

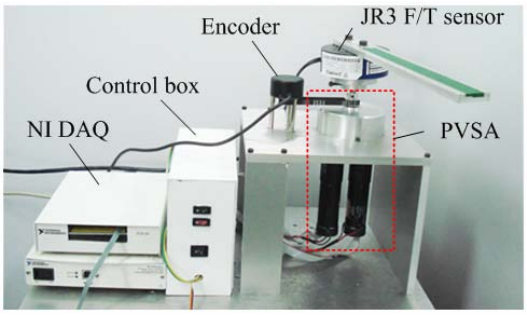

Fig. 8. Experimental setup for stiffness measurement of PVSA.

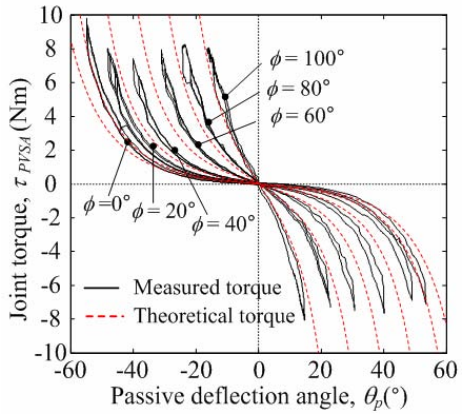

Fig. 9. Experimental results of joint torque versus passive deflection angle of the PVSA.

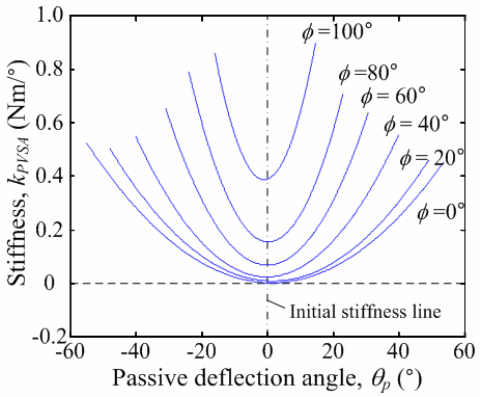

Fig. 10. Experimental results of joint stiffness versus passive deflection angle of the PVSA.

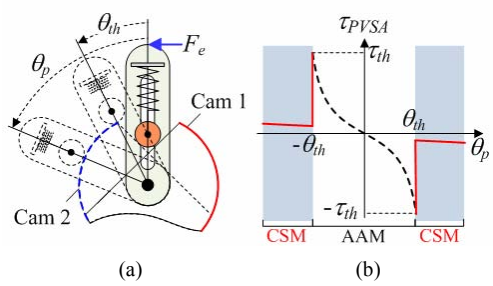

Fig. 11. Collision safety mechanism of PVSA: (a) hybrid cam-profile and (b) τ-θ_p plot of cam in PVSA.

To investigate the joint stiffness variation, the measured torque values shown in Fig. 9 were curve-fitted using a third-order polynomial, and were differentiated with respect to θ_p. As shown in Fig. 10, the initial joint stiffness at a zero passive deflection angle increased nonlinearly even though the position difference ϕ of cam 1 and 2 increased linearly. This characteristic helps provide a wide range of stiffness variation. The minimum initial stiffness was almost zero, and the maximum initial stiffness was about 0.4 Nm/°.

5. Collision safety of the PVSA

5.1 Collision safety function of the PVSA

For collision safety between a robot and a human, the joint stiffness must decrease immediately after an unexpected collision so that the collision force can be absorbed. To satisfy this requirement, the proposed PVSA includes a passive mechanism for collision safety. Compared to the other variable stiffness actuators based on antagonistic actuation, the joint stiffness of the PVSA can be reduced faster than others because it is mechanically decreased instantaneously. The characteristic of collision safety depends on the shape of the cam profile.

The collision safety mechanism works as illustrated in Fig. 11(a). If the torque transmitted to a joint exceeds a predetermined threshold torque τ_{th}, then the follower rotates beyond the threshold angle θ_{th}. At the point of θ_{th}, the cam profile contacting the follower is changed from a linear shape to a curved shape. As a result, the joint torque of the PVSA is discontinuously decreased as shown in Fig. 11(b). The slope of the plot in the collision safety mode (CSM) is much lower than the slope in the antagonistic actuation mode (AAM).

The curved profile for collision safety can be described as $r = ae^{b\theta_p}$, which is a logarithmic spiral as illustrated in Fig. 12(a). The parameters a and b are arbitrary positive real constants of the logarithmic spiral, and the derivative of r is proportional to b. The logarithmic spiral has the property that the angle ψ between the tangent and the radial line at the point (r, θ_p) is constant (i.e., $\psi = \arctan(1/b)$). Thus, θ_c is defined as the angle between the tangent of the spiral and the normal direction of the output link, is ($\pi/2$-ψ).

Spring force F_{cs} is proportional to the amount of compression in spring Δd (= d'-d), where d and d' are the initial and final positions of the follower. Assume that θ_c is small and that $d' = |r| + r_f$. Then, reactive force F_r is obtained in the manner described in Sec. 3.2:

$$\begin{aligned} F_r &= F_{cs} \sin\theta_c \cos\theta_c \\ &= \tfrac{1}{2} k_s (|r| + r_f - d + l_{preset}) \cdot \sin 2\theta_c \end{aligned} \tag{8}$$

where k_s is the spring constant and l_{preset} is the initial compression length of the spring. Therefore, the joint torque in colli-

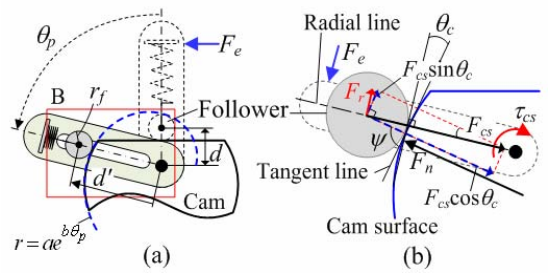

Fig. 12. Cam-follower mechanism of PVSA: (a) curved profile for collision safety and (b) free body diagram of follower (enlarged view of B).

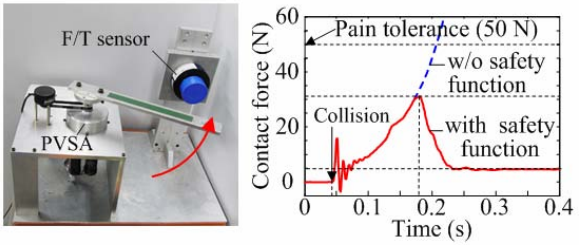

(a) (b)

Fig. 13. Experiments on collision safety: (a) test setup for collision safety and (b) experimental results.

sion safety mode τ_{cs} can be derived as

$$\tau_{cs} = \tfrac{1}{2}k_s(|r| + r_f - d + l_{preset})\sin 2\theta_c \cdot (|r| + r_f) \quad (9)$$

where $r = ae^{b\theta_p}$. Finally, the stiffness k_{cs} of the joint in the collision safety mode is obtained by

$$k_{cs} = \tfrac{1}{2}k_s \cdot (2|r| + 2r_f - d + l_{preset}) \cdot |r'| \cdot \sin 2\theta_c \quad (10)$$

The joint stiffness is significantly decreased due to the small angle θ_c, which generates reactive torque in the cam-follower mechanism.

5.2 Experiments on collision safety

The safety mechanism of the PVSA was verified through collision experiments, as shown in Fig. 13. The collision force between an output link (27 cm in length) and the wall was measured by an F/T sensor installed at the fixed wall. The output link collided against the wall at a speed of 80°/s. The contact force rapidly increased in the antagonistic actuation mode. Without the collision safety function, the contact force easily exceeded the pain tolerance force due to high joint stiffness. However, the contact force did not exceed the threshold force with the collision safety function although the output link was continually actuated (the passive deflection angle in the collision safety mode was ±45°).

The threshold torque of the PVSA was determined by substituting the threshold angle θ_{th} for θ_p in Eq. (3). The threshold torque of the PVSA τ_{th} was 9 Nm when θ_{th} was 60°. The antagonistic actuation mode was switched to the collision safety mode at 0.18 s. The contact force decreased from about 33 N to 5 N, which is well below the pain tolerance. This means that the safety mechanism in the PVSA can absorb collision force effectively without a sensor.

6. Conclusion

A parallel-type variable stiffness actuator (PVSA) was proposed to provide simultaneous control of position and stiffness at the same joint. A dual cam-follower mechanism was adopted to implement antagonistic actuation in the PVSA. Experiments on stiffness variation and unexpected collision were conducted to evaluate the performance of variable stiffness and collision safety of the PVSA, respectively. From this research, the following conclusions are drawn:

(1) The PVSA simultaneously controlled position and stiffness at the same joint by antagonistic actuation.

(2) The PVSA varied the stiffness of the joint from 0 to 0.9 N·m/°, and the response time for the stiffness change was about 0.7 s.

(3) The cam-follower mechanism, which replaced nonlinear springs with linear springs, makes it possible to have flexibility in designing a variable stiffness unit.

(4) The PVSA can immediately change the joint stiffness to a very low value when an external force greater than a predetermined threshold occurs. Thus, it offers collision safety without an expensive joint torque sensor.

Acknowledgment

This work was supported by the Center for Autonomous Intelligent Manipulation under the Human Resources Development Program for Convergence Robot Specialists and by Basic Science Research Program through the National Research Foundation of Korea (No. 2010-0001647).

References

[1] H. J. Lee and S. Jung, Guidance control of a wheeled mobile robot with human interaction based on force control, *International Journal of Control, Automation, and System*, *8* (2) (2010) 361-368.

[2] G. Tonietti, R. Schiavi and A. Bicchi, Design and control of a variable stiffness actuator for safe and fast physical human/robot interaction, *Proc. of the IEEE Int. Conf. on Robotics and Automation*, (2005) 526-531.

[3] R. Schiavi, G. Grioli, S. Sen and A. Bicchi, VSA-II: a novel prototype of variable stiffness actuator for safe and performing robots interacting with humans, *Proc. of the IEEE Int. Conf. on Robotics and Automation*, (2008) 2171-2176.

[4] J. W. Hurst, J. E. Chestnutt and A. A. Rizzi, Design and philosophy of the BiMASC, a highly dynamic biped, *IEEE International Conference on Robotics and Automation*, (2007) 1863-1868.

[5] K. Koganezawa, Antagonistic control of multi-DOF joint by using the actuator with non-linear elasticity, *Proc. of the IEEE International Conference on Robotics and Automation*, (2006) 2201-2207.

[6] F. Daerden, D. Lefeber, B. Verrelst and R. V. Ham, Pleated pneumatic artificial muscles: compliant robotic actuators, *Proc. of the IEEE Int. Conf. on Intelligent Robotics and Systems*, (2001) 1958-1963.

[7] B. Vanderborght, B. Verrelst, R. V. Ham, M. V. Damme and D. Lefeber, A pneumatic biped: experimental walking results and compliance adaptation experiments, *Proc. of the IEEE-RAS International Conference on Humanoid Robotics*, (2005) 44-49.

[8] T. Morita and S. Sugano, Development and evaluation of seven DOF MIA ARM, *Proc. of the IEEE international Conference on Robotics and Automation*, (1997) 462-467.

[9] R. V. Ham, B. Vanderborght, M. V. Damme, B. Verrelst and D. Lefeber, MACCEPA: the mechanically adjustable compliance and controllable equilibrium position actuator for controlled passive walking, *Proc. of the IEEE International Conference on Robotics and Automation*, (2006) 2195-2200.

[10] S. Wolf and G. Hirzinger, A new variable stiffness design: matching requirements of the next robot generation, *Proc. of the IEEE International Conference on Robotics and Automation*, (2008) 1741-1746.

[11] B. S. Kim, J. J. Park and J.-B. Song, Double Actuator Units with Planetary Gear Train for a Safe Manipulator, *Proc. of the IEEE International Conference on Robotics and Automation*, (2007) 1146-1151.

[12] B. S. Kim, J.-B. Song and J. J. Park, A serial-type dual actuator unit with planetary gear train: basic design and applications, *IEEE/ASME Transaction on Mechatronics*, 15 (1) (2010) 108-116.

[13] B. S. Kim and J.-B. Song, Hybrid dual actuator unit: a design of a variable stiffness actuator based on an adjustable moment arm mechanism, *Proc. of the IEEE International Conference on Robotics and Automation*, (2010) 1655-1660.

[14] J. H. Yoo, M. W. Hyun, J. H. Choi, S. C. Kang and S. J. Kim, Optimal design of a variable stiffness joint in a robot manipulator using the response surface method, *Journal of Mechanical Science and Technology*, 23 (2009) 2236-2243.

Ki-Hoon Nam received the B.S. and M.S. degrees in Mechanical Engineering from Korea University in 2008 and 2010, respectively. He is currently an Assistant Engineer of the Manufacturing Technology Center at Samsung Electronics. His research interest includes variable stiffness actuators.

Byeong-Sang Kim received the B.S. degree in Mechanical Engineering from Korea University in 2004. He is currently a Ph.D. candidate in Mechanical Engineering at Korea University. His research interests include design and control of the variable stiffness actuators.

Jae-Bok Song received the B.S. and M.S. degrees in Mechanical Engineering from Seoul National University in 1983 and 1985, respectively, and the Ph. D. degree in Mechanical Engineering from MIT in 1992. He joined the faculty of the School of Mechanical Engineering, Korea University in 1993. Currently, he is a director of Intelligent Robotics Research Center at Korea University. He is also an editor for International Journal of Control, Automation and Systems. His current research interests include safe manipulators, design and control of robotic systems, and mobile robot navigation.